Powder Technology 346 (2019) 171–179

Contents lists available at ScienceDirect

Powder Technology

journal homepage: www.elsevier.com/locate/powtec

Simulation of granular mixing in a static mixer by the discrete element method

Filipp Göbel [a], Shahab Golshan [b], Hamid Reza Norouzi [c], Reza Zarghami [b,*], Navid Mostoufi [b]

[a] Technical University of Munich, Department of Chemistry, Lichtenbergstrasse 4, D-85748 Garching b. München, Germany
[b] Process Design and Simulation Research Centre, School of Chemical Engineering, College of Engineering, University of Tehran, P.O. Box 11155/4563, Tehran, Iran
[c] Department of Chemical Engineering, Amirkabir University of Technology (Tehran Polytechnic), PO Box: 15875-4413, Hafez 424, Tehran, Iran

ARTICLE INFO

Article history:
Received 16 October 2018
Received in revised form 19 January 2019
Accepted 8 February 2019
Available online 11 February 2019

Keywords:
Revolving static mixer
Kenics
Ross LPD
DEM
Particle mixing
RSD

ABSTRACT

Mixing of solids in static mixers with different geometries was studied using discrete element method (DEM) simulations. The DEM code was validated by comparing the simulation results with experimental data for a static mixer with 180° Kenics elements. Two different types of blending elements, Kenics and LPD, were considered and compared. Effects of the number of blending elements, the angle of twist of Kenics elements, the slope angle of LPD elements and particle to tube diameter ratio were studied on efficiency, mechanism and time of mixing. Flow patterns of solids in the mixers were investigated with the aid of the velocity field of particles, granular temperature and velocity gradient. It was shown that the average solids flow rate decreased from 101.8 g/s to 54.2 g/s when number of blending elements increased from 2 to 5. On the other hand, the mixing efficiency improved with increasing the number of elements from two to four at a constant number of passes. The results of simulations revealed that the Kenics elements with the twist angle of 150° and 180° and LPD elements with the angle of slope of 60° have the best performance in terms of mixing quality and mixing time. It was also found that larger values of tube diameter (smaller d/D) lead to a better performance of static mixers. Hybrid arrangement of elements (a combination of Kenics and LPD elements in one mixer) significantly weakens the performance of the static mixer.

© 2019 Elsevier B.V. All rights reserved.

1. Introduction

Mixing of different kinds of particles is an essential operation in many industries. Achieving a homogeneous mixture of particles is essential for product quality assurance and is mainly obtained by combining the convective and/or dispersive mixing mechanisms [1,2]. The flow pattern of the granular material is very complex due to the coexistence of particles with various shapes, densities, and sizes in a single system. Also, the time dependent phenomena, like segregation and adhesion, add to this complexity. Hence, this behavior is not well understood yet [3]; and finding a general theory than can describe the rheology and flow characteristics of granular flows is still a big challenge [4,5]. To solve this problem, laboratory experiments [2,7] or detailed numerical simulations [6–8] have been performed for each individual process.

Granular mixers are classified into batch and continuous mixers. From the operational point of view, continuous mixers offer better stability and homogeneity in comparison with batch mixers [9]. The vast range of available continuous mixers, from common to customized ones, makes it difficult to choose a proper type for a designated task. The most common type of solid mixer is the one with a single shaft that rotates blending elements in the mixer. These mixers usually differ in the shape and configuration of the blending elements [3]. The continuous shaft mixers provide a high level of mixing and can handle a large throughput. However, the problems with such mixers is that they consume a high amount of energy during the operation and attrition is sometimes a problem due to sever contact between rotating elements and particles [3].

Static mixer is another type of continuous solid mixer. In this type, the mixing occurs due to the flow of the solid through stationary and fixed elements in a tube. Since the mixing process does not need additional energy input, this type of mixer is advantageous over other continuous mixers [10]. The required energy of mixing in a static mixer is supplied only by the flow of particles (in many conditions by gravity) [11]. Static mixers offer a very short residence time, low shear rates and a self-cleaning structure [10]. The process of mixing involves repeated splitting, spreading and transporting pockets of the particle flow [12]. Generally, static mixers offer smaller dimensions as well as lower costs of equipment and maintenance [10]. They are commonly used as premixing units, but can also replace conventional continuous mixers entirely [12]. For the design of a static mixer, the type of blending elements, the number of those elements and the velocity of particle flow are decisive [11].

* Corresponding author.
E-mail address: rzarghami@ut.ac.ir (R. Zarghami).

https://doi.org/10.1016/j.powtec.2019.02.014
0032-5910/© 2019 Elsevier B.V. All rights reserved.

Despite the importance of static mixers and their potential in the simultaneous handling and mixing of granular flows, a little research is done in the field [13–15]. Ghanem et al. [13] listed available commercial static mixers. One of them is the Kenics static mixer (Chemineer Inc.), in which blending elements have a blade twist of 180°, as shown in Fig. 1 (a). Another type is the LPD mixer (Ross Engineering Inc.), illustrated in Fig. 1(b). Jovanovic et al. [11] and Pezo et al. [12] simulated granular flow in a revolving static mixer using discrete element method (DEM) coupled with computational fluid dynamics (CFD). They investigated the mixing quality and the influence of revolutions of a static mixer with three Kenics elements.

Most of the knowledge for mixer design is obtained by either experiments or modeling. Between these two, modeling has shown to be a promising tool to understand granular flows, to optimize the parameters of the mixing process, and to reduce the need for experimental work [16]. The DEM is a reliable and efficient approach for the modeling of granular flow. This modeling approach has been utilized to investigate various mixing processes, ranging from fluidized beds to shaft batch and continuous mixers [17–25]. In the present work, DEM simulation of a static mixer was carried out and validated by experimental results available in the literature. Then, effects of mixer geometry on mixing efficiency and mixing mechanisms were discussed. Two different types of blending elements (Kenics and LPD) were examined with various geometric configurations (number of blending elements, the angle of twist and slope). The influence of particle to tube diameter ratio was also investigated. This work offers the first basic knowledge for sizing and designing static mixers for granular particles.

2. Models and methods

2.1. Static mixers

As shown in Fig. 1, a static mixer is generally composed of a cylindrical tube and some blending elements, which are fixed one above another with a twist angle to stimulate mixing. Two types of blending elements, Kenics and LPD, were considered in this study. Dimensions of the static mixer and blending elements are listed in Table 1.

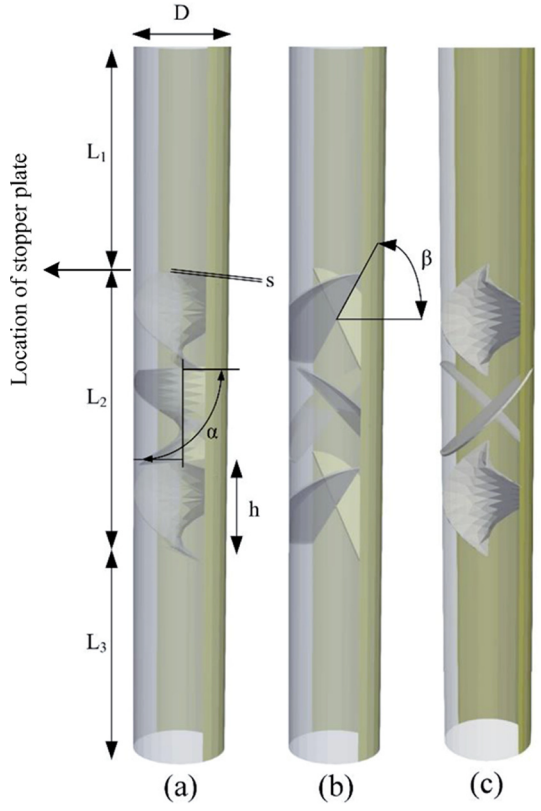

Fig. 1. Geometry of the static mixer setup (a) 180° Kenics, (b) 45° LPD and (c) hybrid.

In the Kenics-type mixer, the mixing zone consists of three Kenics elements with an axial twist angle of $\alpha = 180°$. This setup was considered as the base design for the Kenics-type mixer and was used for validation in this work. The twist angle of 180° represents the commercially available type of the Kenics element [10]. Effect of the twist angle was also studied in Kenics mixers with the twist angles of 90°, 150°, and 210°. Effects of the number of the mixing elements and particle diameter to tube diameter ratio were also investigated.

In the LPD-type mixer, the performance of a mixer with the LPD blending elements was evaluated. In the base case, shown in Fig. 1(b), the slope angle, β, was 45°. Effect of varying the slope angle between 30° and 60° was also evaluated. The details of these simulations are given in Table 1. In addition, a hybrid static mixer, consisting of two 180° Kenics elements on the top and bottom and one 45° LPD element in the middle (illustrated in Fig. 1(c), was considered as a combination of those two types.

The list of simulation conditions is given in Table 2. The first four simulations are aimed to investigate the effect of the number of elements, ranging from 2 to 5 Kenics elements with the twist angle of 180°. In the next nine simulations, a static mixer setup with a constant number of three blending elements was considered. They can be split up into three series of simulations: Kenics static mixers with various twist angles of 90° to 210°, LPD static mixer with slope angles between 30° and 60°, a simulation for hybrid static mixer, and two simulations (simulations 8 and 9 in Table 2) with different particle to tube diameter ratios (d/D from 0.02 to 0.0417).

Experiments were performed in a short static mixer and the mixer was consecutively rotated to simulate a longer mixer [12]. Each rotation (180°) was called "a pass." In each pass, the particles were allowed to settle in the bottom. After that, the whole assembly was rotated by 180° to start the next pass. The same procedure was also followed in the DEM simulations. In the simulation, rotation of the setup was simulated by reversing the direction of the gravitational acceleration after each pass was finished.

2.2. Discrete element method

For describing the dynamics of granular flow of in the static mixer, the soft-sphere DEM simulation was used. Governing equations for translational and rotational motions in this method are [26]:

$$m_i \frac{dv_i}{dt} = \sum_j \left(F_{ij}^N + F_{ij}^T\right) + m_i g \tag{1}$$

$$I_i \frac{d\omega_i}{dt} = \sum_j M_{ij}^T + M_{ij}^r \tag{2}$$

Table 1
Geometric parameters of static mixers and blending elements.

Parameter	Unit	Symbol	Value
Static mixer tube			
Length	mm	L	540
Diameter	mm	D	60
Kenics blending element			
Height	mm	h	60
Thickness	mm	s	1.5
Twist angle	°	α	90, 150, 180, 210
LPD blending element			
Height	mm	h	36, 60, 100
Thickness	mm	s	1.5
Angle of slope	°	β	30, 45, 60

Table 2
Simulation conditions for different static mixers.

No.	Element type	No. of elements	Twist angle α (°)	Angle of slope β (°)	Mixing zone (cm)	d/D	t_p (s)	Flow rate (g/s)
1	Kenics	2	180	–	120	0.0417	1.88	101.8
2	**Kenics**	**3**	**180**	**–**	180	**0.0417**	**2.46**	**77.8**
3	Kenics	4	180	–	240	0.0417	2.95	64.9
4	Kenics	5	180	–	300	0.0417	3.53	54.2
5	Kenics	3	90	–	180	0.0417	1.07	178.9
6	Kenics	3	150	–	180	0.0417	2.02	94.8
7	Kenics	3	210	–	180	0.0417	3.32	57.7
8	Kenics	3	180	–	180	0.03	2.1	91.2
9	Kenics	3	180	–	180	0.02	1.71	112.0
10	LPD	3	–	30	180	0.0417	9.79	19.6
11	**LPD**	**3**	**–**	**45**	180	**0.0417**	**4.03**	**47.5**
12	LPD	3	–	60	210	0.0417	2.26	84.7
13	Hybrid	3	180	45	180	0.0417	3.19	60.0

Normal and tangential forces, F^N and F^T, are calculated by the viscoelastic contact theory [27–29]:

$$F_{ij}^N = \left[\left(-\frac{4}{3}E_{eff}\sqrt{R_{eff}}\delta_N^{3/2}\right) - \left(\tilde{\eta}_N\delta_N^{1/4}v_{rN}\right)\right]n_{ij} \tag{3}$$

$$F_{ij}^T = -\frac{16}{3}\,G_{eff}\sqrt{R_{eff}}\delta_N^{1/2}\delta_T t_{ij} \tag{4}$$

where

$$E_{eff} = \left(\frac{1-\nu_i^2}{E_i} + \frac{1-\nu_j^2}{E_j}\right)^{-1} \tag{5}$$

$$R_{eff} = \left(\frac{1}{R_i} + \frac{1}{R_j}\right)^{-1} \tag{6}$$

$$G_{eff} = \left(\frac{2-\nu_i}{G_i} + \frac{2-\nu_j}{G_j}\right)^{-1} \tag{7}$$

in which E, G, ν, and R are the Young's modulus, shear modulus, Poisson's ratio, and radius of the particle, respectively, with subscript i and j referring to contacting particles.

If during a contact, the Coulomb's criterion ($|F_{ij}^T| \geq \mu|F_{ij}^N|$) is violated, gross sliding occurs and the tangential overlap, δ_T, is limited based on the following equation [30]:

$$\delta_T = \operatorname{sgn}(\delta_T)\frac{\mu\left|F_{ij}^N\right|}{k_T} \tag{8}$$

where

$$k_T = \frac{16}{3}G_{eff}\sqrt{R_{eff}\delta_N} \tag{9}$$

Tangential and rolling friction torques are obtained by [31]:

$$M_{ij}^T = R_i n_{ij} \times F_{ij}^T \tag{10}$$

$$M_{ij}^r = -\mu_r R_i \mid F_{ij}^N \mid \frac{\omega_i - \omega_j}{\mid \omega_i - \omega_j \mid} \tag{11}$$

where μ_r is the rolling friction factor.

The simulations were performed using LIGGGHTS open-source code [32].

2.3. Data treatment

Simulation results were further processed to obtain the granular temperature, the velocity gradient and the relative standard deviation (RSD). Granular temperature is the mean square of velocity fluctuations of particles and is calculated according to the following equation [17]:

$$\theta = \frac{1}{3}\sqrt{\left[\overline{U'^2_x} + \overline{U'^2_y} + \overline{U'^2_z}\right]} \tag{12}$$

Here, U' is the velocity fluctuation of particles relative to their local average velocity with the subscript denoting the direction. Granular temperature provides information about the significance of diffusive mechanism of mixing. For calculating the granular temperature in the static mixer, the volume was divided into 9000 ($15 \times 15 \times 40$) hexagonal cells. For this division, the mixer body (cylinder) was embeded (sorrounded) with a cuboid. This cuboid was divided into 9000 cells in the Cartesian coordinates. Consequently, the size of each cell would be 4 mm (x) × 4 mm (y) × 13.5 (z) mm. It should also be mentioned that the cell dimensions were chosen adequately small such that the size would not affect the results. In each time step, the average particle velocity and the fluctuation of the particle velocity were calculated in each cell and the granular temperature was then evaluated by Eq. (12). In these calculations, cells with particles less than ten were omitted.

Beside the granular temperature, which is an indicator of the diffusive mixing, velocity gradient was also evaluated to determine the influence of shear mechanism on the mixing process. To calculate the velocity gradient, the off-diagonal components of the axial particle velocity gradient tensor in the z-direction was evaluated. Only z-direction was considered since the dominant flow of particles in the static mixer is in this direction. The magnitude of velocity gradient in the static mixer was calculated from:

$$\chi = \left|\frac{\partial u_z}{\partial x}\right| + \left|\frac{\partial u_z}{\partial y}\right| \tag{13}$$

To evaluate the derivatives of particle velocity, the average velocity of particles, evaluated for obtaining the granular temperature, was used. It should also be mentioned that the same hexagonal cells (was explained previously) were used to calculate the velocity gradient distribution in the mixer. In other words, the values of Δx and Δy were to 4 mm in this case.

RSD was used for assessing the mixing quality. This parameter is defined as follows [11]:

$$RSD = 100\,\frac{\sigma}{\overline{\overline{C}}} \tag{14}$$

$$\sigma = \sqrt{\frac{\sum_{i=1}^{n}\left(\overline{C} - C_i\right)^2}{n-1}} \tag{15}$$

The concentration C_i of one kind of particles was computed in each cell (those containing 10 or more particles) and the average concentration of all cells, $\overline{C}$ was then evaluated [33].

3. Results and discussion

In total, 13 DEM simulations were carried out for studying the mixing efficiency in different static mixers. The simulation setups are listed in Table 2. Simulations 2 and 11 (bold in Table 2) are the base designs for Kenics and LPD static mixers, respectively. The simulation parameters are listed in Table 3. The parameters were taken from Pezo et al. [11,12], from which the results were used for validation in this work. The initial packed bed was formed by letting all particles to

Table 3
DEM simulation parameters [9].

Parameter	Symbol	Value
Particle density (kg/m^3)	ρ	650
Particle diameter (mm)	d	2.5
Young's modulus (Pa)	E	10^7
Poisson's ratio	ν	0.25
Coefficient of restitution	e	0.5
Rolling friction coefficient	μ_r	0.3
Static friction coefficient	μ	0.3
Time step (s)	Δt	5×10^{-6}
Simulation time (s)	–	25[a]

[a] Simulation time reported here correspond to setup No. 10 in Table 2.

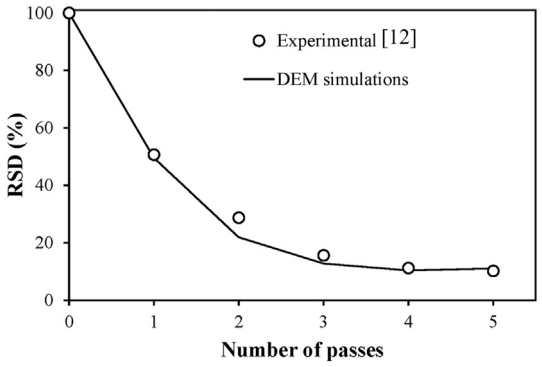

Fig. 2. RSD values as a function of number of passes in 180° Kenics static mixer.

settle down by gravity from top of the static mixer tube, above the blending elements in the upper compartment (on top of the mixing zone). For this purpose, a stopper plane was utilized at this point in the simulations. This stopper was removed at the start of the simulations. Location of this stopper plate is also illustrated on Fig. 1. It should also be mentioned that bottom and top of the mixer body were closed in the simulations. After the insertion and settling of particles, they are divided into two types based their location (half left and half right). In the attached video (simulation of mixing of particles in the static mixer), these two types can be observed distinctly with red and blue colors. In the calculation of the mixing quality (which is performed by using RSD here), these two types were utilized. When all particles were settled, they were allowed to fall into the lower compartment while passing through the mixing zone. Then, after the first pass was finished, the gravity vector was instantaneously reversed and the particles passed the mixing zone for the second time. This gravity reversion was repeated four times after the particles were settled down to simulate five passes in a revolving static mixer [12]. An animation clip, showing all five passes for simulation setup 2 (see Table 2, base design for Kenics static mixer), can be found in the supplementary materials. Depending on the setup of the static mixers, the time of a single pass was between 1.07 s to 9.79 s. This time, t_p, is averaged over the five passes and listed in Table 2. The flow rates of particles in the static mixers were calculated based on t_p, using the following equation:

$$flow\ rate = \frac{V_s \rho}{t_p} \tag{16}$$

in which V_s (≈ 0.000295 m^3) and ρ show the total volume of solids in the mixer and the density of particles, respectively. Besides the mixing quality in the static mixer, the flow rate of solids is a critical parameter in the evaluation of the performance of these mixers.

3.1. Validation

The experimental results of Pezo et al. [12] were used to validate the DEM model in this study. Experimental and simulated RSD values against the number of passes for the 180° Kenics static mixer with three blending elements are shown in Fig. 2. The decaying trend of RSD to about 10% after five passes displays the good quality of mixing achieved in the mixer. It can be seen in this figure that the RSDs obtained from simulations are in good agreement with the experimental values. Based on this good agreement, it can be concluded that the DEM code used in the present study is valid and can be used to study the effect of design geometry and find the optimum design of static mixers.

3.2. Flow pattern

Velocity field, granular temperature and velocity gradient were evaluated for 180° Kenics and 45° LPD static mixers (three blending elements each). To obtain the velocity field, the mean velocity vector for each cell was calculated in each time step, then averaged over time for a single pass. The resulting velocity field is shown in Fig. 3 for both mixers. The mean velocity in the Kenics base design (highlighted in Table 2) clearly increases while passing through the mixing zone. Particles reach the maximum mean velocity upon exiting the third blending element when falling into the lower compartment. A reason for this trend could be the helical geometry of the Kenics elements that does not notably hinder the downward motion of particles due to the gravitational acceleration. In contrast, in the LDP base design (highlighted in Table 2), the maximum mean velocity occurs between the first and the second elements and the flow follows a zigzag pattern. In contrast to the Kenics elements, LPD elements change the flow direction of particles drastically due to the rectangular alignment of the blades. This drastic change of the flow direction prevents particles to accelerate significantly while falling down. The particles collide the surface of the second

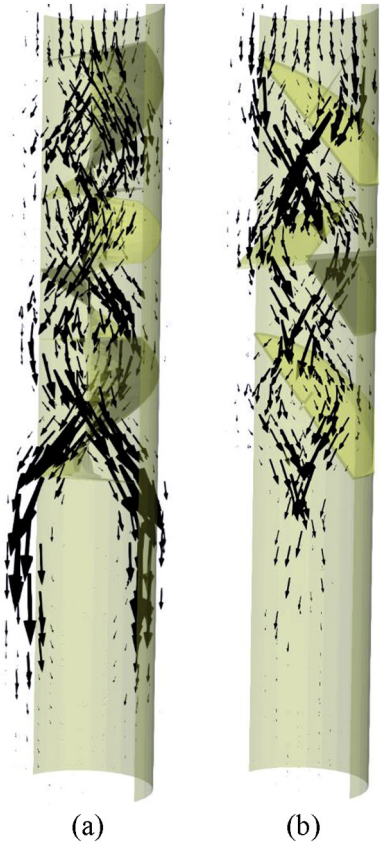

Fig. 3. Time averaged velocity fields (a) 180° Kenics static mixer (b) 45° LPD static mixer.

and third element perpendicularly (≈ 90°), thereby lose some of their kinetic energy. This trend cannot be observed in the Kenics elements. This is reflected in the solid flow rate passing through the static mixer, another important design parameter in continuous mixers. The solid flow rate in the Kenics-type mixer is almost 1.6 times that in the LPD-type mixer (see Table 2).

The granular temperatures of the above mentioned static mixer setups are illustrated in Fig. 4 for the Kenics mixer and in Fig. 5 for the LPD mixer. Three vertical-sectional planes at different depths (at depths of 0, 14.4 and 21.9 mm from the half cross section), as well as nine cross-sectional planes (at heights of 0.18, 0.2, 0.22, 0.24, 0.26, 0.28, 0.3, 0.32 and 0.34 m) at different heights, are shown in these figures. The granular temperatures are averaged over time for one pass through the mixing zone. It can be seen in Fig. 4 that the granular temperature takes its highest value slightly above the surface of the second and the third elements and decreases again towards the wall and the center of the static mixer. A completely different distribution of granular temperature can be seen in the case of LPD mixer in Fig. 5. The peak values can be found in the upper part of the mixing zone. This trend also can be attributed to higher magnitude of velocity field vectors in that section of the mixing zone. In fact, higher velocity of particles leads to higher velocity fluctuations when particles face an obstacle where a change in the direction of their motion happens. Furthermore, a higher granular temperature can be observed in the path between the successive elements. Especially, in the area of collision of particles with wall elements (associated with a change in flow direction), the values of granular temperature rise due to the chaotic movement of particles. A high granular temperature indicates a better mixing performance due to diffusion [17].

There are mechanisms of particle mixing, including diffusion, shear and convection. The rate of shear mechanism can be approximated by the velocity gradient. The velocity gradients in Kenics and LPD base designs are illustrated in Figs. 6 and 7, respectively (the same conditions as in Figs. 4 and 5). These figures indicate that the highest values of velocity gradient can be found in the regions with the largest velocity field vectors (see Fig. 3). This trend continues to the end of the mixing zone in the case of Kenics type elements. However, the maximum shear is only observed in the space between blending elements in the LPD mixer. In general, the shear rate is high in the regions where the flow of particles with high velocity is affected/deflected by the wall and hence the mixing due to the shear mechanism. Comparing Figs. 6 and 7, the maximum values of the velocity gradient in the LPD static mixer are lower (more than four times) compared to the Kenics setup, but concentrated within the mixing zone in contrast to its end and lower compartment for the Kenics type. In addition, a larger fraction of the mixing zone of Kenics mixer shows noticeable shear rate. Therefore, the share of shear mixing in the Kenics mixer is larger than that in the LPD mixer.

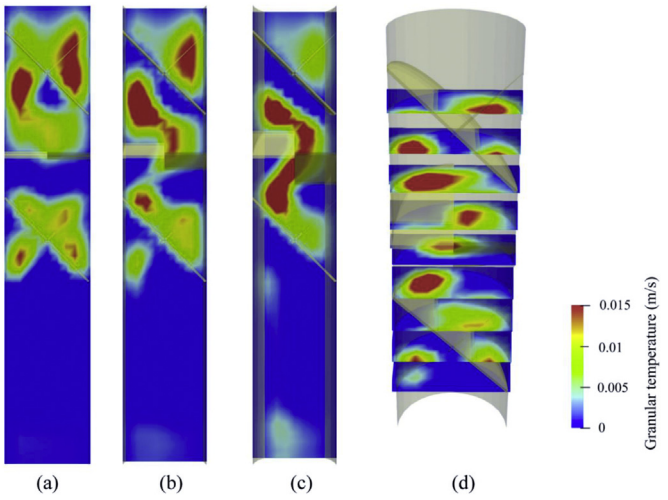

Fig. 5. Granular temperature in 45° LPD static mixer (a - c) vertical and (d) horizontal slices.

3.3. Effect of number of blending elements

The number of blending elements can affect both mixing quality and the solid flow rate passing the mixer. Fig. 8 shows RSD against the number of passes for the 180° Kenics static mixer with 2 to 5 blending elements. The RSD per pass decreases (mixing efficiency improved) with increasing the number of elements from two to four at a constant number of passes and there is no noticeable difference between four and five blending elements. The same behavior was observed in the experiments of Bauman et al. [34] in a similar Kenics mixer. The solid flow rates reported in Table 2 shows that the average solid flow rate in the mixer is 101.8 g/s for the mixer with two blending elements. This value decreases to 54.2 g/s as the number of blending elements is increased to 5. When the number of blending elements is increased in the mixer, the number of obstacles against the free flow of particles in the tube increases which acts as a resistance to the flow of particles.

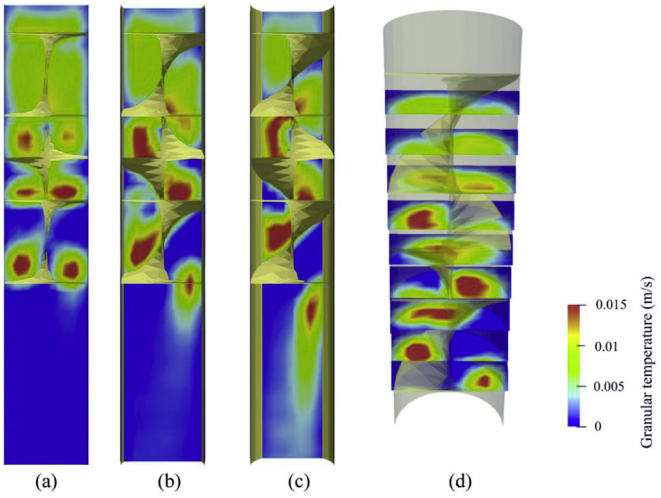

Fig. 4. Granular temperature in 180° Kenics static mixer (a - c) vertical and (d) horizontal slices.

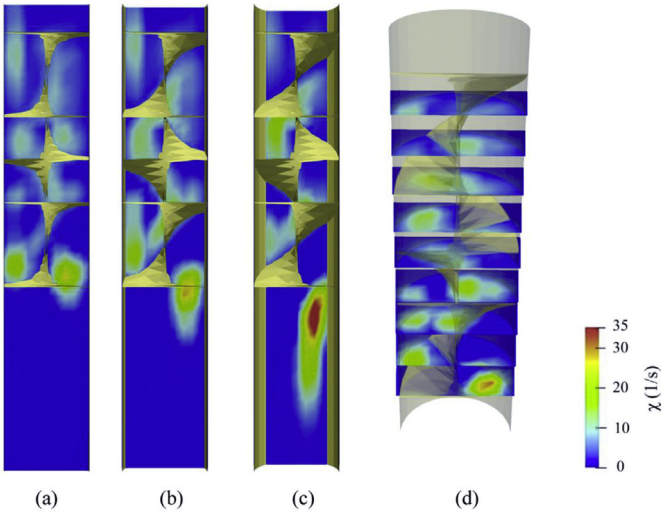

Fig. 6. Velocity gradient in 180° Kenics static mixer (a - c) vertical and (d) horizontal slices.

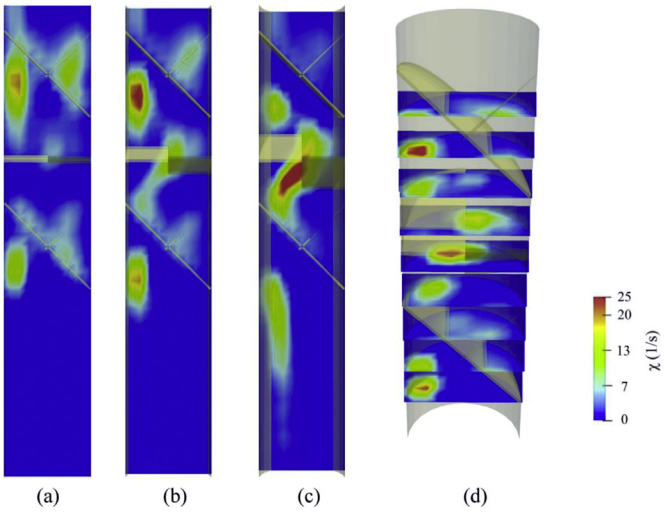

Fig. 7. Velocity gradient in 45° LPD static mixer (a - c) vertical and (d) horizontal slices.

Fig. 8 also demonstrates that the RSD decreases (mixing quality increases) with the number of passes in all cases. For the mixer with four or five blending elements, this final value of RSD is reached after two passes while it attained after three passes for the mixer with three blending elements and finally it is obtained after four passes for the mixer with two elements. To explain these trends, it seems that the utilization of more than four elements is not necessary to reach the maximum quality of mixing. Consequently, considering both the mixing quality and the flow rate passing the mixer, a mixer with three or four blending elements can be an optimum choice for the static mixer studied in these simulations.

3.4. Effect of angle of blending elements

The angle at which the blending elements are fixed to the wall can also influence the mixing quality and solid flow rate through the mixer. For this reason, the twist angle (α) in the Kenics mixer was varied between 90° and 210° and the angle of slope (β) in the LPD mixer was varied between 30° and 60°.

Fig. 9 shows the variation of RSD in the Kenics mixer with various twist angles as a function of the number of passes. The twist angle of the Kenics element has a significant influence on the mixing quality. For example, at a constant number of passes (here two passes), the RSD is 59.8% for $\alpha = 90°$ and decreases to 43.5% for $\alpha = 150°$ and then to 21.9% for $\alpha = 180°$. This trend shows that the twist angle of 180° has the best performance in achieving a higher quality of mixing, followed by twist angles of 210° and 150° the twist angle of 90° of Kenics elements by far shows the worst mixing efficiency. This trend matches the results of Thakur, Vial, Nigam, Nauman, Djelveh [10] on the mixing of fluids in Kenics mixer in which the mixer with the twist angle of 180° provided the best mixing efficiency. It can be concluded that the mixing improves when the flow is repeatedly divided and recombined by mixing elements as the particle flow passes the mixing elements. However when the twist angle deviates from 180°, a fraction of particles escape the process of flow division and recombination. Such escapes of particles (similar to a bypass flow), decrease the quality of particle mixing after passing the mixing element. The more deviation from 180°, a larger fraction of particles bypasses the mixing process, which decreases the mixing quality. By comparing the flow rates reported in Table 2, it can be found that the particle flow rate increases as the twist angle of Kenics elements is decreased. Based on these results, to obtain the maximum mixing efficiency and maintaining the flow rate of particles high after five passes, the Kenics elements with the twist angle of 150° and 180° seem to be the best choice in this type of mixer. It should be mentioned that these reported best twist angles (150° and 180°) were chosen based on both mixing quality and flowrate (mixing time) in the mixer.

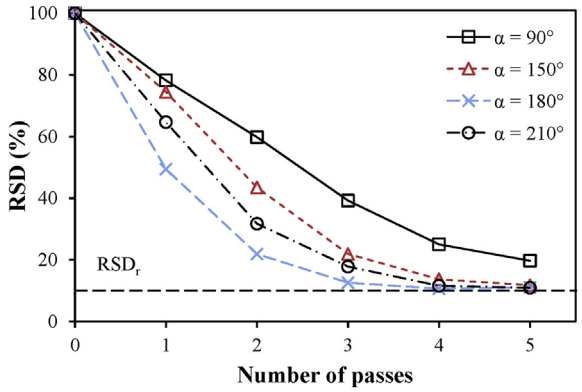

Fig. 9. RSD results for static mixers with Kenics elements in different twist angles α.

A similar analysis was performed for the LPD mixing elements in the mixer with three angles of slope ($\beta = 30°$, 45° and 60°). Fig. 10 shows the variation of RSD in the LPD mixer at various angles of slope as a function of the number of passes. The angle of slope does not affect the RSD in the mixer noticeably. The particle flow rate passing through the LPD mixer is 84.7 g/s for the slope angle of 60° while it decreases to 19.6 g/s as the slope angle is decreased to 30°. The reason for this trend is that decreasing the angle of

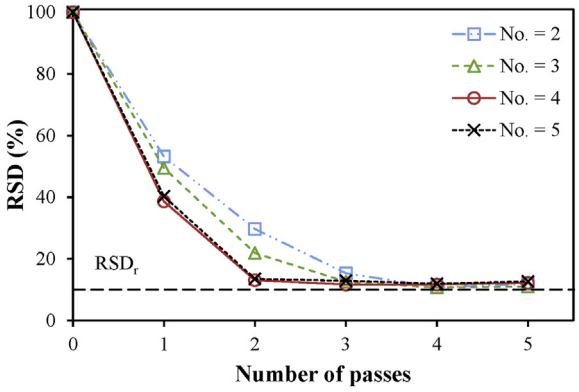

Fig. 8. Comparison of the RSD values over the number of passes for a 180° Kenics static mixer with 2 to 5 blending elements.

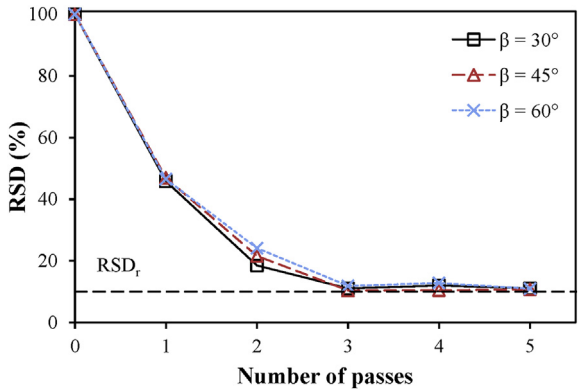

Fig. 10. RSD results for static mixers with LPD elements in different angles of slope β.

slope decreases the available space for the flow of particles which in turn reduces the particle flow rate. Considering both mixing quality and flow rate of particles, the angle of slope of 60° is preferable for LPD elements.

3.5. Effect of particle to tube diameter ratio

The particle diameter remained constant in all the simulations of this work. For investigating the effect of particle to tube diameter ration on the mixing efficiency, diameter of the static mixer with three Kenics elements (both mixer body and Kenics elements) was increased from the base case ($D = 60$ mm, $d/D = 0.0417$) to $D = 83.3$ mm ($d/D = 0.03$, simulation 8 in Table 2) and $D = 125$ mm ($d/D = 0.02$, simulation 9 in Table 2). Fig. 11 shows the variation of RSD as a function of the number of passes for various d/D values. During the first two passes, increasing the tube diameter improves the mixing quality slightly. During the first pass, the RSD decreases to 49.5% and 37.9% for $D = 60$ mm and $D = 125$ mm, respectively. As the size and the total number of particles were kept the same, the larger mixing zone can take more particles and mix the particles more effectively. However, the three mixers perform the same as the number of passes exceeds three. The particle flow rate increases with increasing the tube diameter (see Table 2). This trend is expected since the cross section area for flow of particles increases with the tube diameter which in turn increases the flow rate of particles. Based on these results, larger values of tube diameter (smaller d/D) are preferable in static mixers, at least in the range of values studied in the present work. It should be mentioned that the effect of particle size on the mixing behavior requires further research and in this work only the effect of the mixer size (which affects d/D) has been studied.

3.6. Type of blending element

A comparison between the two investigated blending element types in their base design (180° Kenics and 45° LPD) is shown in Fig. 12. The RSD graphs for these static mixers follow an almost identical trend. The solid flow rate passing through the Kenics mixer is 77.8 g/s while it is 47.5 g/s in the LPD mixer (see Table 2). This comparison demonstrates better overall performance of the Kenics mixer. In fact, both mixer types result in a similar mixing quality while the Kenics mixer produces less resistance against the solid flow.

A hybrid static mixer was also tested by simulation in the present investigation. The hybrid mixer is a mixer with two 180° Kenics element (top and bottom) and one 45° LPD element (middle). Evolution of the RSD over the number of passes in this mixer is also shown in Fig. 12. It can be seen in this figure that the RSD for the hybrid mixer is around 10% more than the corresponding values

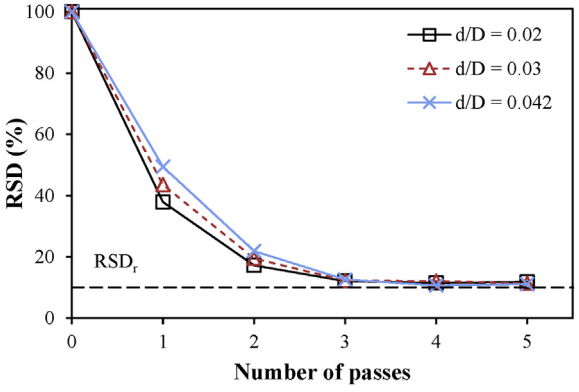

Fig. 11. RSD results for 180° Kenics static mixers in different particle to tube diameter ratios d/D.

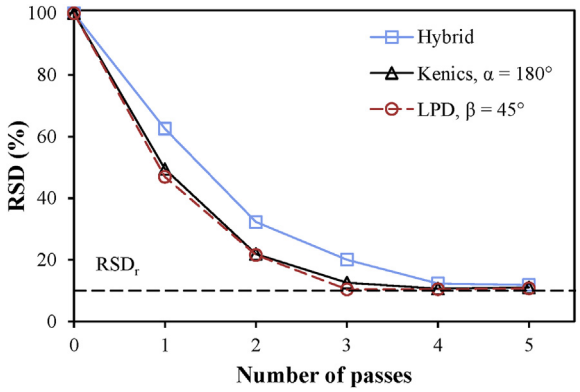

Fig. 12. RSD results for a hybrid static mixer with two 180° Kenics and one 45° LPD blending element.

for the base designs during passes one to three. In passes four and five, the difference in RSD values almost disappears and the final mixing limit is again attained in all mixers. The reason for this trend is that difference might be found in the various flow and mixing patterns of the Kenics or LPD static mixer. The latter (LPD) shows a slower mean velocity but achieves almost the same mixing quality as the Kenics base design, which has a more developed velocity field (see Fig. 3). The combination of these different blending elements could lead to a disturbance of the specific mixing pattern of each element type, thus affects the mixing performance negatively. The granular temperature and velocity gradient in a horizontal sectional plane in the center of the hybrid static mixer are visualized in Fig. 13. The granular temperature notably shows fewer hotspots across the mixing zone in comparison with the two base designs (see Figs. 4 and 5), which could be linked to the uncoordinated velocity fields of different elements (LPD and

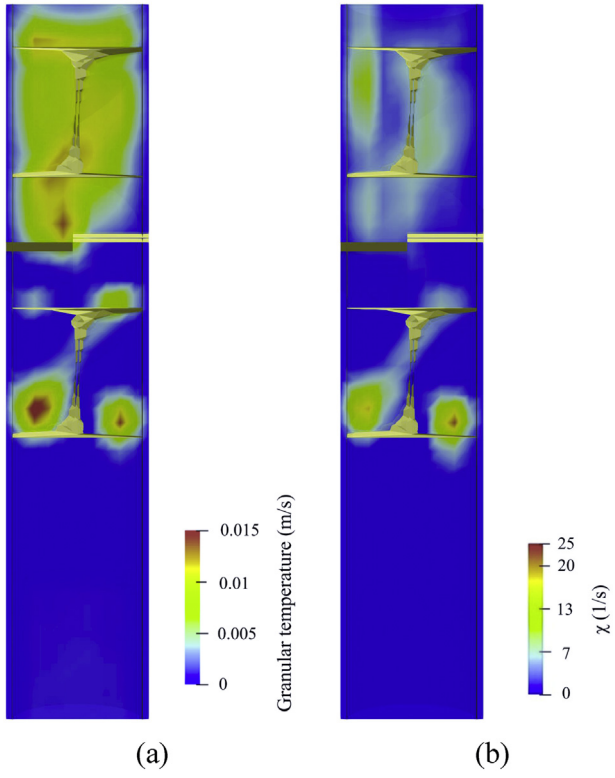

Fig. 13. (a) Granular temperature and (b) velocity gradient for the hybrid static mixer.

Kenics), which leads to longer time required for a single pass. The average time $t_p = 3.19$ s for a single pass lies between the corresponding values of the two base designs (see Table 2). The lower granular temperature during mixing can be responsible for higher RSD values. In addition, the velocity gradient in Fig. 13(b) has no remarkable deviation from the two base designs (see Figs. 6 and 7). Therefore, it cannot be responsible for the difference in the mixing efficiency between hybrid and base designs.

4. Conclusions

Discrete element method simulations of static mixers were performed in the present work. Results of simulations were validated with the experimental data from literature. It was observed that the simulation results are in good agreement with the experimental data. Effects of mixer geometry (number of blending elements, angle of twist, angle of slope and particle to tube diameter ratio) on mixing efficiency, mixing mechanism and mixing time were studied. Two different types of blending elements, Kenics and LPD, were utilized in the mixers. The flow pattern of solids in the mixers was investigated using the velocity field of particles, granular temperature (which represents the diffusion mechanism of mixing) and velocity gradient (which represents the shear mechanism of mixing). It was observed that the average solids flow rate decreased constantly from 101.8 g/s to 54.2 g/s for mixers with 2 to 5 blending elements, while the mixing efficiency improved with increasing the number of elements from two to four at a constant number of passes and no noticeable difference was found between four and five blending elements. Results of simulations on the effect of twist and slope angles revealed that to obtain the maximum mixing efficiency and maintaining the flow rate of particles high, the Kenics elements with the twist angle of 150° and 180° and LPD elements with the angle of slope of 60° are the best choices. It was also illustrated that using a larger tube diameter value (smaller d/D) leads to the better performance of static mixers. By comparing the mixing efficiencies and flow rates of static mixers with different geometries, it was concluded that the Kenics mixer with four elements at twist angle of 180°, and LPD mixer with three elements at slope angle of 60° illustrate the best performance in terms of quality of mixing and flow rate. A hybrid arrangement of elements (a combination of Kenics and LPD elements in one mixer) was also tested in the simulations and it was observed that the hybrid arrangement weakens the quality of mixing.

Notation

D	diameter of tube, mm
d	diameter of particles, mm
E	Young's modulus, Pa
e	coefficient of restitution, dimensionless
F_{ij}^N	normal force, N
F_{ij}^T	tangential force, N
G	shear modulus, Pa
g	gravity acceleration, m/s^2
h	height of blending element, mm
I	moment of inertia, kg.m^2
L	length of static mixer tube, mm
L_1	length of upper compartment, mm
L_2	length of mixing zone, mm
L_3	length of lower compartment, mm
M_{ij}^T	tangential torque, N.m
M_{ij}^r	rolling friction torque, N.m
m	mass of particle, kg
N	total number of particles, dimensionless
n	number of samples, dimensionless
n_{ij}	normal vector, dimensionless
R^2	correlation coefficient, dimensionless
R	radius of particles, mm
RSD	relative standard deviation, %
s	thickness of blending element, mm
t	time, s
t_{ij}	tangential vector, dimensionless
U'	fluctuating velocity, m/s
V_s	total volume of solids in the mixer, m^3
v	velocity of particle, m/s
x	concentration, dimensionless
$\bar{x}$	average concentration, dimensionless

Greek letters

α	twist angle of the Kenics element, deg
β	angle of slope of the LPD element, deg
Δt	time step, s
δ	overlap of particles, m
$\tilde{\eta}_n$	damping coefficient, kg/s.m.$^{0.25}$
θ	granular temperature, m^2/s^2
μ	friction coefficient, dimensionless
μ_r	rolling friction coefficient, dimensionless
ν	Poisson's ratio, dimensionless
ν_{rN}	relative velocity of particle in normal direction, m/s
ρ	density of particles, kg/m^3
χ	velocity gradient, 1/s
ω	angular velocity of particle, rad/s

Subscripts and superscripts

0	initial state
eff	effective
i, j	particles i and j
N	normal direction
p	passing
r	random mixture
T	tangential direction
x, y, z	Cartesian vector components

Supplementary data to this article can be found online at https://doi.org/10.1016/j.powtec.2019.02.014.

Acknowledgments

Financial supports from the National Elites Foundation of Iran for Postdoc researchers (Allameh Tabatabaei prize) are sincerely acknowledged.

References

[1] D. Ponomarev, V. Mizonov, H. Berthiaux, C. Gatumel, J. Gyenis, E. Barantseva, A 2D Markov chain for modelling powder mixing in alternately revolving static mixers of Sysmix® type, Chem. Eng. Process. Process Intensif. 48 (2009) 1495–1505.
[2] M. Zhan, G. Sun, Y. Lu, X. Wang, Y. Zhang, Characterization of mixing of binary particles in a continuous colliding static mixer, Powder Technol. 291 (2016) 448–455.
[3] M. Jiang, Y. Zhao, G. Liu, J. Zheng, Enhancing mixing of particles by baffles in a rotating drum mixer, Particuology 9 (2011) 270–278.
[4] J. Bridgwater, Mixing of powders and granular materials by mechanical means—a perspective, Particuology 10 (2012) 397–427.
[5] E.L. Paul, V.A. Atiemo-Obeng, S.M. Kresta, Handbook of Industrial Mixing: Science and Practice, John Wiley & Sons, 2004.
[6] X. Bednarek, S. Martin, A. Ndiaye, V. Peres, O. Bonnefoy, Extrapolation of DEM simulations to large time scale application to the mixing of powder in a conical scrunknown, Chem. Eng. Sci. 197 (2019) 223–234.
[7] M. Ebrahimi, A. Yaraghi, F. Ein-Mozaffari, A. Lohi, The effect of impeller configurations on particle mixing in an agitated paddle mixer, Powder Technol. 332 (2018) 158–170.
[8] M.K. Saeed, M.S. Siraj, Mixing study of non-spherical particles using DEM, Powder Technol. 128 (2018) 195–204.
[9] S. Muerza, H. Berthiaux, S. Massol-Chaudeur, G. Thomas, A dynamic study of static mixing using on-line image analysis, Powder Technol. 128 (2002) 195–204.
[10] R. Thakur, C. Vial, K. Nigam, E. Nauman, G. Djelveh, Static mixers in the process industries—a review, Chem. Eng. Res. Des. 81 (2003) 787–826.

[11] A. Jovanović, M. Pezo, L. Pezo, L. Lević, DEM/CFD analysis of granular flow in static mixers, Powder Technol. 266 (2014) 240–248.
[12] M. Pezo, L. Pezo, A. Jovanović, B. Lončar, R. Čolović, DEM/CFD approach for modeling granular flow in the revolving static mixer, Chem. Eng. Res. Des. 109 (2016) 317–326.
[13] A. Ghanem, T. Lemenand, D. Della Valle, H. Peerhossaini, Static mixers: mechanisms, applications, and characterization methods–a review, Chem. Eng. Res. Des. 92 (2014) 205–228.
[14] H. Gussefeld, Static Mixer for Flowing Media, Google Patents, 1977.
[15] H. Hiorth, Continuous Flow Static Mixer for Mixing Powder and/or Suspension Materials with Liquid Materials, Google Patents, 1980.
[16] H. Zhu, Z. Zhou, R. Yang, A. Yu, Discrete particle simulation of particulate systems: a review of major applications and findings, Chem. Eng. Sci. 63 (2008) 5728–5770.
[17] S. Golshan, R. Zarghami, H.R. Norouzi, N. Mostoufi, Granular mixing in nauta blenders, Powder Technol. 305 (2017) 279–288.
[18] N. Gui, J. Yan, W. Xu, L. Ge, D. Wu, Z. Ji, J. Gao, S. Jiang, X. Yang, DEM simulation and analysis of particle mixing and heat conduction in a rotating drum, Chem. Eng. Sci. 97 (2013) 225–234.
[19] M. Halidan, G. Chandratilleke, S. Chan, A. Yu, J. Bridgwater, Prediction of the mixing behaviour of binary mixtures of particles in a bladed mixer, Chem. Eng. Sci. 120 (2014) 37–48.
[20] X. Hua, J. Curtis, Y. Guo, B. Hancock, W. Ketterhagen, C. Wassgren, The internal loads, moments, and stresses in rod-like particles in a low-speed, vertical axis mixer, Chem. Eng. Sci. 134 (2015) 581–598.
[21] H. Ma, Y. Zhao, Modelling of the flow of ellipsoidal particles in a horizontal rotating drum based on DEM simulation, Chem. Eng. Sci. 172 (2017) 636–651.
[22] H.R. Norouzi, R. Sotudeh-Gharebagh, N. Mostoufi, Segregation behaviour of particles in gas solid fluidized beds at elevated pressure, J. Chem. Petrol. Eng. 46 (2012) 111–121.
[23] O. Olaofe, A. Patil, N. Deen, M.A. van der Hoef, J. Kuipers, Simulation of particle mixing and segregation in bidisperse gas fluidized beds, Chem. Eng. Sci. 108 (2014) 258–269.
[24] S. Yang, Y. Sun, L. Zhang, J.W. Chew, Impact of granular segregation on the solid residence time and active-passive exchange in a rotating drum, Chem. Eng. Sci. 173 (2017) 287–302.
[25] S. Yang, Y. Sun, L. Zhang, J.W. Chew, Segregation dynamics of a binary-size mixture in a three-dimensional rotating drum, Chem. Eng. Sci. 172 (2017) 652–666.
[26] H.R. Norouzi, R. Zarghami, R. Sotudeh-Gharebagh, N. Mostoufi, Coupled CFD-DEM Modeling: Formulation, Implementation and Application to Multiphase Flows, John Wiley & Sons, 2016.
[27] A. Di Renzo, F.P. Di Maio, An improved integral non-linear model for the contact of particles in distinct element simulations, Chem. Eng. Sci. 60 (2005) 1303–1312.
[28] H.R. Hertz, Uber die Beruhrung fester elastischer Korper und Uber die Harte, Verhandlung des Vereins zur Beforderung des GewerbefleiBes, Berlin, 1882 449.
[29] Y. Tsuji, T. Tanaka, T. Ishida, Lagrangian numerical simulation of plug flow of cohesionless particles in a horizontal pipe, Powder Technol. 71 (1992) 239–250.
[30] N. Maw, J. Barber, J. Fawcett, The oblique impact of elastic spheres, Wear 38 (1976) 101–114.
[31] Y. Zhou, B. Wright, R. Yang, B.H. Xu, A.-B. Yu, Rolling friction in the dynamic simulation of sandpile formation, Phys. A Stat. Mech. Appl. 269 (1999) 536–553.
[32] C. Kloss, C. Goniva, A. Hager, S. Amberger, S. Pirker, Models, algorithms and validation for opensource DEM and CFD–DEM, Prog. Comput. Fluid Dynam. Int. J. 12 (2012) 140–152.
[33] M. Lemieux, G. Léonard, J. Doucet, L.-A. Leclaire, F. Viens, J. Chaouki, F. Bertrand, Large-scale numerical investigation of solids mixing in a V-blender using the discrete element method, Powder Technol. 181 (2008) 205–216.
[34] I. Bauman, D. Ćurić, M. Boban, Mixing of solids in different mixing devices, Sadhana 33 (2008) 721–731.